



OPEN ACCESS

EDITED BY

Daniele Dini,
Imperial College London, United Kingdom

REVIEWED BY

Saša Milojević,
University of Kragujevac Faculty of Engineering,
Serbia
Milan Bukvic,
Faculty of Engineering, University of Kragujevac,
Serbia

*CORRESPONDENCE

Michael Pusterhofer,
✉ michael.pusterhofer@unileoben.ac.at

RECEIVED 30 July 2024

ACCEPTED 16 January 2025

PUBLISHED 17 February 2025

CITATION

Pusterhofer M, Maier M, Scharf R, Haumer F and Grün F (2025) Hydrodynamic performance testing of artificial textures using a novel pin-on-disc test method.
Front. Mech. Eng. 11:1473028.
doi: 10.3389/fmech.2025.1473028

COPYRIGHT

© 2025 Pusterhofer, Maier, Scharf, Haumer and Grün. This is an open-access article distributed under the terms of the [Creative Commons Attribution License \(CC BY\)](https://creativecommons.org/licenses/by/4.0/). The use, distribution or reproduction in other forums is permitted, provided the original author(s) and the copyright owner(s) are credited and that the original publication in this journal is cited, in accordance with accepted academic practice. No use, distribution or reproduction is permitted which does not comply with these terms.

Hydrodynamic performance testing of artificial textures using a novel pin-on-disc test method

Michael Pusterhofer*, Michael Maier, Raphael Scharf, Florian Haumer and Florian Grün

Chair of Mechanical Engineering, Montanuniversität Leoben, Leoben, Austria

In times of global climate change, the reduction in friction in technical applications is of crucial significance. Surface textures are one possibility for reducing friction in lubricated contacts. To provide a deeper understanding of the effects of surface textures on the tribological performance, this study analyzes wedge-shaped, textured lubrication gaps using a novel test rig with an *in situ* lubrication gap height measurement. Using this experimental pin-on-disc setup, chevron-shaped and cylindrical textures with two different heights ($h_t = 10$ and $50 \mu\text{m}$) were tested under full-film lubrication conditions. The pin was tilted in a very precise way to generate a convergent lubrication gap. The test results show the potential for friction reduction using textures. In general, it can be stated that the investigated textures show clearly different behavior compared to the smooth reference specimens. Mostly, a reduction in friction force was measured for the texture specimens, which was accompanied by a reduction in the lubrication gap height. The system still operates in full-film lubrication, but there is a higher risk of entering the mixed-friction regime. In summary, no universal performance trend for single textures can be stated; it needs to be checked for each specific operating point which texture provides the best enhancement.

KEYWORDS

SRV tribometer, pin-on-disc, surface texture, friction reduction, hydrodynamic

1 Introduction

Textures are not a new concept for surfaces with fluids flowing around them. Nature shows that certain geometries can improve friction performance compared to ideally smooth surfaces. For example, the unique geometry of fish scales minimizes drag, thereby enabling efficient locomotion of the species (Wu et al., 2021; Luo et al., 2015). In flora nature has also revolutionized leaf surfaces with the hydrophobic and self-cleaning lotus effect (Zhang et al., 2016).

Efficiency-enhancing efforts and sustainability are key functions in times of global climate change. Approximately one-fourth of the world's energy consumption is required to overcome friction in tribological contacts (Holmberg and Erdemir, 2017). Therefore, systematic texturing of surfaces is used by humans in a variety of technical applications to increase their efficiency. For example, special coatings and surface topographies in pipelines can reduce friction losses (Luo et al., 2015; Liu et al., 2020). Furthermore, geometries oriented in the streamline direction, so-called riblets, are used to reduce friction losses on airplanes. Friction savings of 5%–8% can be achieved in this way (Luo et al., 2015). Riblets are also used to increase the power of wind turbines (Leitl et al., 2020). However, surface texturing is also used in non-technical applications, such as swimming suits or golf balls. However, the understanding of the effects leading to drag

reduction during the flight of a golf ball is not yet completely understood (Chowdhury et al., 2016). It should also be mentioned that modifications of the fluids, e.g., by applying nanocomposites, can lead to significant friction reductions (Bukvic et al., 2024).

In lubricated contacts, modifying the surface topography is one way to increase efficiency, along with reduced oil viscosity and intermistic stops. The honing structure of internal combustion engines is one example of the performance enhancement of textures (Milojevic et al., 2023; Milojevic et al., 2022; Milojevic and Stojanovic, 2018). In the last 50 years, various experimental and simulative research studies have been carried out in the field of surface texturing. Depending on the operating conditions, the texture geometry can have positive or negative effects on the resulting hydrodynamic friction and normal forces (Dobrica et al., 2010; Mishra and Ramkumar, 2018; Morris et al., 2015; Scharf et al., 2024a). Furthermore, for similar geometrical textures, the depth, texture density, and position of the textured area are essential for the hydrodynamic forces (Morris et al., 2015; Rosenkranz et al., 2019). However, the exact mechanisms responsible for the increase in normal force are still controversial today: the original explanation for the load support was cavitation (Hamilton et al., 1966), but this is insufficient according to the current state of the art (Dobrica et al., 2010; Gropper et al., 2016). Furthermore, the inertial forces, particularly, vortices in dimples, are argued to cause the pressure build-up (Sahlin et al., 2005). Dobrica and Fillon (2009) contradicted this and explained that inertial effects have a negative impact on the pressure buildup. Either an additional or reduced load capacity due to convective inertia effects, depending on the texturing geometry, was observed by de Kraker et al. (2010). Another mechanism for increasing the pressure build-up is referred to as inlet suction. Thereby, it is argued that due to a diverging lubrication gap area, the lubricant supply in the contact zone is increased, which increases the pressure build-up (Fowell et al., 2006; Olver et al., 2006).

To gain a basic understanding of tribo-contacts, model tests are a useful tool (Milojevic et al., 2024; Goti et al., 2020; Skulic et al.,

2024). In recent years, the influence of textures on the hydrodynamic conditions in the lubrication gap has been evaluated using different experimental test configurations. Pin-on-disc test configurations have been used to determine the influence of texture form (Bijani et al., 2018), dimensional ratios (Babu et al., 2021), density (Babu et al., 2021; Liu et al., 2019), and operating conditions (Bijani et al., 2018; Babu et al., 2021; Liu et al., 2019) for parallel sliding contacts. Azami et al. (2022) also used a pin-on-disc arrangement to test line and point contacts. In addition to friction reduction, wear reduction in the mixed friction regime was observed with a textured disc. Texture geometries based on natural leaves, such as cylindrical roller thrust bearings, also resulted in wear and friction reduction (Long et al., 2021). The investigations showed that the symmetry of the leaves and the density of the side arms have a significant influence on the results (Long et al., 2021). Testing of application-oriented experimental configurations, such as the ring-on-liner setup (Mishra and Ramkumar, 2018; Morris et al., 2015; Pusterhofer et al., 2019) or textured journal-bearing test rigs (Vlădescu et al., 2019; Grützmacher et al., 2018; Filgueira Filho et al., 2021), has also revealed the potential for friction reduction and increased normal forces.

The main focus of this research is to establish a reliable test method for comparing different textures based on their hydrodynamic performance enhancement, specifically in terms of increased normal force and/or reduced friction force. To provide reliable results, which will be essential for future tasks aimed at understanding how textures work, the measurement of the lubrication gap height is crucial along with the measurement of normal and friction forces. Pin specimens with different textures were tested to check the method's screening capability.

2 Materials and methods

Within the framework of this study, a lubrication gap section of 10×10 mm is analyzed. The texture is applied to one surface of the

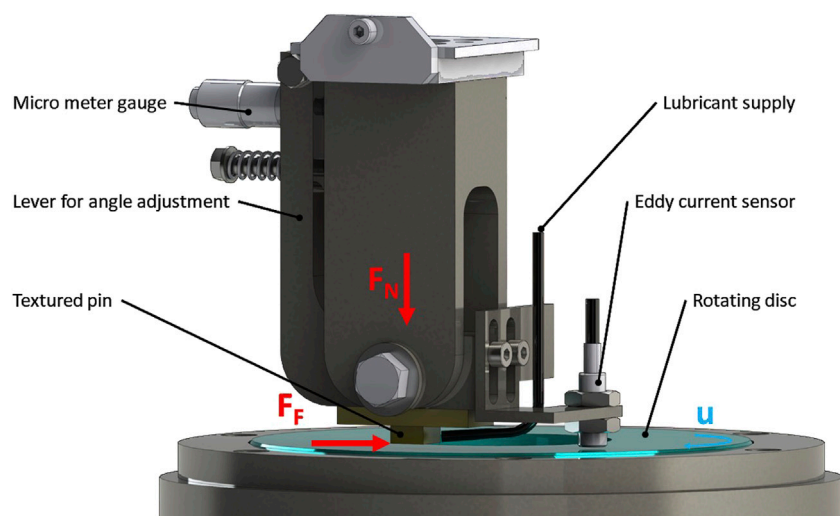


FIGURE 1
Basic setup of the experimental test method.

TABLE 1 Boundary conditions of the SRV5 tribometer.

Load	3–2500 N
Rotational speed	0–2,000 min ⁻¹
Temperature	Room temperature, – 150°C

lubrication gap. For the experimental tests, an SRV5 Multifunctional Tribometer (Optimol Prüftechnik GmbH, Munich, Germany) with a user-made, bespoke pin-on-disc configuration is used. For this purpose, the normal force F_N is applied to the pin, and the associated clear lubrication gap height h_0 and friction force F_F are measured (Figure 1). The boundary conditions for the tribometer in the rotational mode are shown in Table 1.

2.1 Experiment

As shown in Figure 1, the textured pin is pressed vertically onto the rotating disc. The angle α between the textured and rotating surfaces is adjusted using the lever with a micrometer gauge. By applying the lubricant in front of the contact zone, a sufficient lubricant supply is ensured (Figure 2). The rotation speed of the disc is set to 1,136.8 min⁻¹. The eccentric arrangement ($r_{ex} = 42$ mm) between the pin and disc results in a relative speed of 5 m/s.

For the experimental tests, first, the lubricant supply is activated, and then the disc is set into rotation. At the beginning, a minimum normal force F_N (~0.5 N) is set on the tribometer. Due to the hydrodynamic pressure build-up, resulting from the relative speed, the lubrication wedge geometry, and the lubricant viscosity, a certain lubrication gap height h_0 is obtained. This ensures that the two contact surfaces are completely separated from each other and that the normal force on the pin is fully absorbed by the hydrodynamic force in the lubrication gap. Then, the normal force F_N is successively increased on the tribometer, while the relative speed remains constant, which results in a different minimum lubrication gap height h_0 . The normal force is increased up to a level of 26 N, which represents a nominal contact pressure of 0.26 MPa. At no point during the experiment did asperity contact or wear occur, and full-film lubrication was always present. The clear height h_0 is

measured using the eddy current sensor for the different normal forces F_N (Figure 2). The experiments were conducted at room temperature, which was approximately 25°C.

2.2 Test material

The pins are made of aluminum alloy EN AW-6082 (AlSi1MgMn). In addition to a smooth version, two further textures with two different texture heights ($h_t = 10$ μm and 50 μm) (Figure 3) are tested in the experiments. High-precision milling tools are used to produce the textures on the pin surface. The second contact surface, the rotating disc, is made from steel 42CrMo4. Roughness values are provided in Table 2. Lambda values vary between 35 (the maximum occurring lubrication gap height of 45 μm) and 15 (the minimal occurring lubrication gap height of 20 μm).

The details of the manufactured textures are shown in Figure 4. It needs to be pointed out that these textures are not optimized in a preceding simulation process. Therefore, it was initially unclear whether these textures would cause an enhancement or deterioration. The main goal was to provide strongly varying geometry to check the test method's separation properties.

The engine oil, Shell Rimula R5 10 W-30, with a dynamic viscosity of 0.294 Pas and a density of 857.2 kg/m³ at 25 C, is used as the lubricant.

Table 3 provides an overview of the tested textures and the boundary conditions.

2.3 Measurement/test procedure

The hydrodynamic forces F_L and F_D are induced by the flow and the pressure in the lubrication gap. The vertical normal force F_L can be evaluated directly using the load cell integrated into the tribometer. In addition, the friction force F_D is determined from the multichannel force of the Optimol Rotational Module (Optimol Instruments Prüftechnik GmbH, 2024). The temperature in the contact environment is recorded by the integrated measuring unit of the test machine. A specific combination of surface texture, the

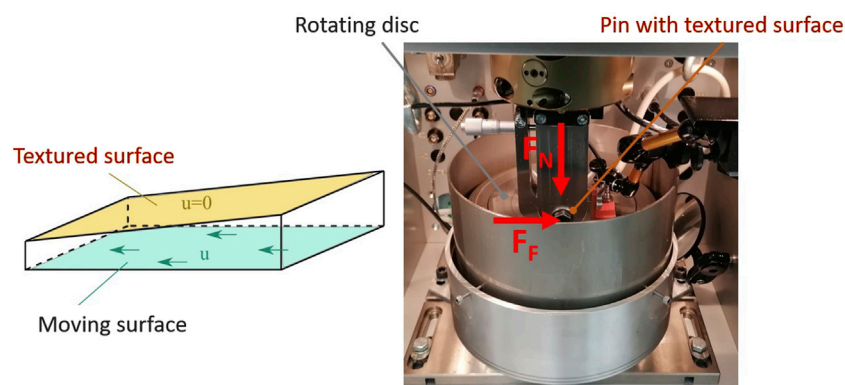


FIGURE 2
Details of the experimental test configuration.

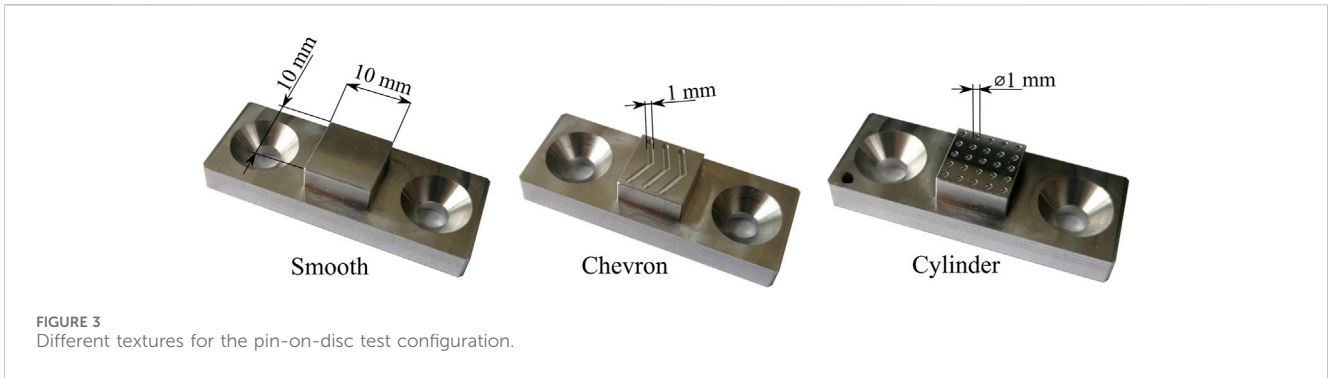


FIGURE 3 Different textures for the pin-on-disc test configuration.

TABLE 2 Roughness values for the test specimens.

	Disc	Pin (smooth)
Ra	1.1 μm	0.3 μm
Rq	1.2 μm	0.4 μm
Rz	4.0 μm	2.0 μm

rotational speed of the disc, used lubricant, and applied vertical load results in a corresponding clearance height h_0 . This is determined using the eddy current sensor ES-S1 (Micro-Epsilon, Ortenburg, Germany) and transferred by an OPC-UA interface option to SRV software.

At the beginning of a test, the specimen first has to be aligned parallel to the disc. This is achieved by pressing the pin onto the stationary disc. For qualitative evaluation of the parallelism of the pin and the disc surface, pressure-sensitive measurement films (Fujifilm Prescale, Tokyo, Japan) are placed between these two surfaces, and the parallelism can be adjusted using a micrometer screw. The alignment perpendicular to the rotational axis of the mounting area of the adapter. For the measurement of the lubrication gap height, the measurement of the initial displacement of the eddy current sensor is recorded at a standstill ($h_0 = 0$).

Finally, the disc is accelerated under nearly load-free conditions, and the lubrication gap reaches its maximum value at the desired relative speed (5 m/s). Then, the vertical load FL is successively increased, and the change in the lubrication gap height h_0 can be measured using the eddy current sensor with a theoretical accuracy of 0.02 μm. The sensor has been calibrated to the disc material (42CrMo4) by the manufacturer to ensure the corresponding measurement accuracy. Furthermore, field calibrations were performed with the installed test rig.

3 Results

3.1 Validation of the experimental method

To check the plausibility of the method, an analytical calculation is used. Based on the Reynolds equation, the approaches detailed by

Lang and Steinhilper (2014), Fuller et al. (1960), and Schiebel and Körner (1933) can be used to calculate the normal force of a smooth, convergent, lubricated wedge. In addition, using the approach described by Vogelpohl (1967), the friction force can be calculated analytically as follows:

$$F_{finite} = \frac{5}{6} \cdot \frac{F_{infinite}}{1 + a \left(\frac{L}{b}\right)^2}$$

$$F_{infinite} = B \frac{6 \cdot \eta \cdot U \cdot L^2}{(h_1 - h_0)^2} \cdot \left(\ln \frac{h_1}{h_0} - 2 \frac{h_1 - h_0}{h_1 + h_0} \right),$$

$$h_1 = h_0 + l \cdot \tan(\alpha),$$

$$a = \frac{10}{(1 + 2m)^2} \left\{ (m + m^2)^2 + \frac{1 - 2 \cdot (m + m^2)}{12 \left[(1 + 2m) \ln \frac{1+m}{m} - 2 \right]} \right\},$$

$$m = \frac{h_0}{h_1 - h_0} = \frac{1}{m'},$$

$$\mu = \frac{4}{5} \cdot \frac{(1 + 2m) \ln \frac{1+m}{m} - 1,5}{\frac{L}{h_0} \cdot \frac{m}{1 + a \left(\frac{L}{b}\right)^2} \left[(1 + 2m) \ln \frac{1+m}{m} - 2 \right]}$$

For all the investigated pitch angles, the analytical solution was applied. Figure 5 shows the result for a pitch angle of 0.3° as blue dots. As can be seen, with an increasing normal force, which was controlled during the experiments, the lubrication gap height decreases. In addition, a decrease in friction force in relation to the normal force can be recognized.

For the reference tests with smooth surfaces, three separate tests were conducted, showing good reproducibility between them. Furthermore, similar trends to those seen in the analytical solution can be observed. However, a discrepancy exists between the analytical and experimental results. Similar mismatches, as shown in Figure 5 for the 0.3° configuration, were found for the other pitch angle configurations. Possible reasons for this mismatch will be analyzed in the “Discussion” section.

3.2 Experimental results

Figures 6–8 depict the results of the experiments with textured pins. For each pitch angle, the results of texture specimens are compared with the corresponding results of smooth pin specimens. It can be observed that there is a clear separation between the different texture geometries and texture depths, as well as a significant separation from the reference results of the smooth pin.

TABLE 3 Overview of the conducted tests.

	Smooth	Chevron		Cylinder	
		10 μm	50 μm	10 μm	50 μm
Texture height	0				
Contact surface	10 × 10 mm				
Pitch angle α	0.2°, 0.3°, 0.4°, 0.5°, 0.75°, 1.0°				
Relative velocity	5 m/s				
Normal force F _N	0.5 up to 30 N				
Temperature	~25°C				

All tests were conducted in full hydrodynamic film lubrication. All tests were started with a low normal force, which corresponds to a high gap height. The maximum applied normal force was chosen in such a way that the gap height did not exceed 20 μm. If one considers the roughness values from Table 2, lambda values are between 35 (maximum occurring lubrication gap height of 45 μm) and 15 (minimal occurring lubrication gap height of 20 μm), which is typical for full-film lubrication.

Figure 6 shows the results for a pitch angle of 0.2° and 0.3°. Comparing the lubrication gap heights, it can be recognized that all textures show a smaller gap height at the same normal force as the smooth reference tests. In this way, a higher risk of entering a mixed friction regime can be assigned.

It is the cylinder texture with a depth of 50 μm that shows the highest gap heights for the tests at 0.2°. In addition, the friction force is lower at a similar normal load than for the smooth reference geometry. This results in a beneficial COF behavior for the cylinder size with 50-μm depth.

The chevron textures with a similar depth of 50 μm depict the lowest gap heights. Friction is in the very range of smooth results. For both texture geometries with smaller depths (10 μm), the lubrication gap heights lay between the two deeper geometries. It

seems that, at least for the gap height, the geometry of the texture, whether a cylinder or a chevron, is important.

For the test with a pitch angle of 0.3°, the lubrication gap height of all textured geometries is much more in the range of the smooth reference geometries. Chevron and cylinder textures with a depth of 50 μm depict a lower gap height, whereas the cylinder texture with 10-μm depth shows the highest gap height. Regarding the friction force, this exact texture (cylinder with 10-μm depth) shows the highest friction force and, consequently, also the highest COF, which lies in the very range of the smooth results. The other textures show lower friction forces at the corresponding normal forces, which leads to lower COF values. The Chevron geometry with a depth of 10 μm, which provides the lowest COF values, seems very beneficial, but it only creates a moderate lubrication gap height reduction.

Figure 7 shows the results for pitch angles α = 0.4° and 0.5°. The trend continues, where, with an increasing pitch angle, the lubrication gap heights of the textured specimens approach those of the smooth reference tests. For a pitch angle of 0.4°, the shallower textures (chevron and cylinder with 10-μm depth) have the higher gap height, followed by a higher friction force and COF. Cylinder textures provide slightly higher values (gap height, friction force, and COF) than the chevron texture with 10-μm depth. For this pitch angle, again, the chevron geometry with a depth of 10 μm is the one that provides the best combination of friction reduction and moderate gap height reduction.

The situation for a pitch angle of 0.5° seems much more complex. The highest gap height is provided by chevron textures with 10-μm depth. However, for friction force and COF, this texture does not provide such a clear trend and lies more in the middle of the results. This is in agreement with the previous results that the chevron geometry with 10-μm depth is a very good compromise between friction reduction and bearing capacity. The lowest gap height for the investigation at a pitch angle of 0.5° is provided by the 50-μm-deep chevron texture; however, contrary to the trend, this not only provides the lowest friction but also the highest friction

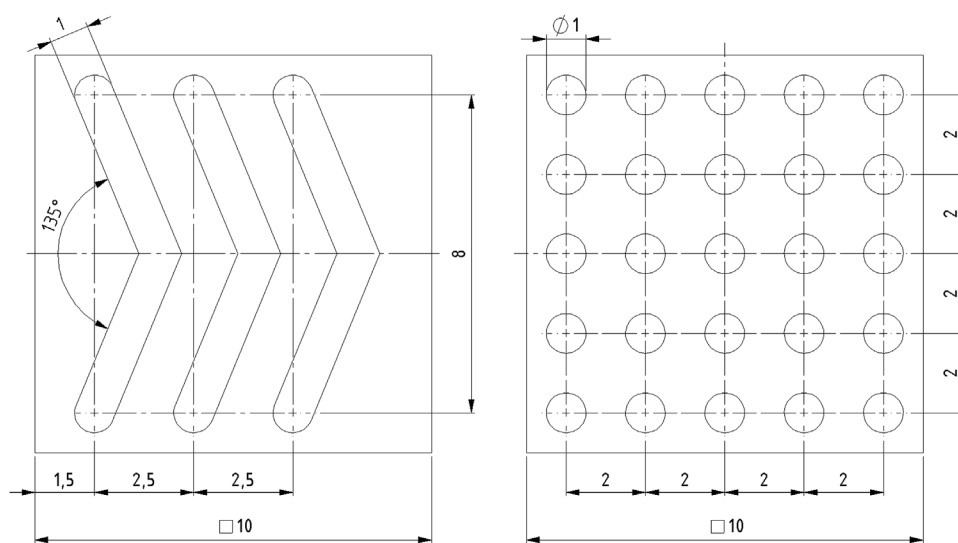
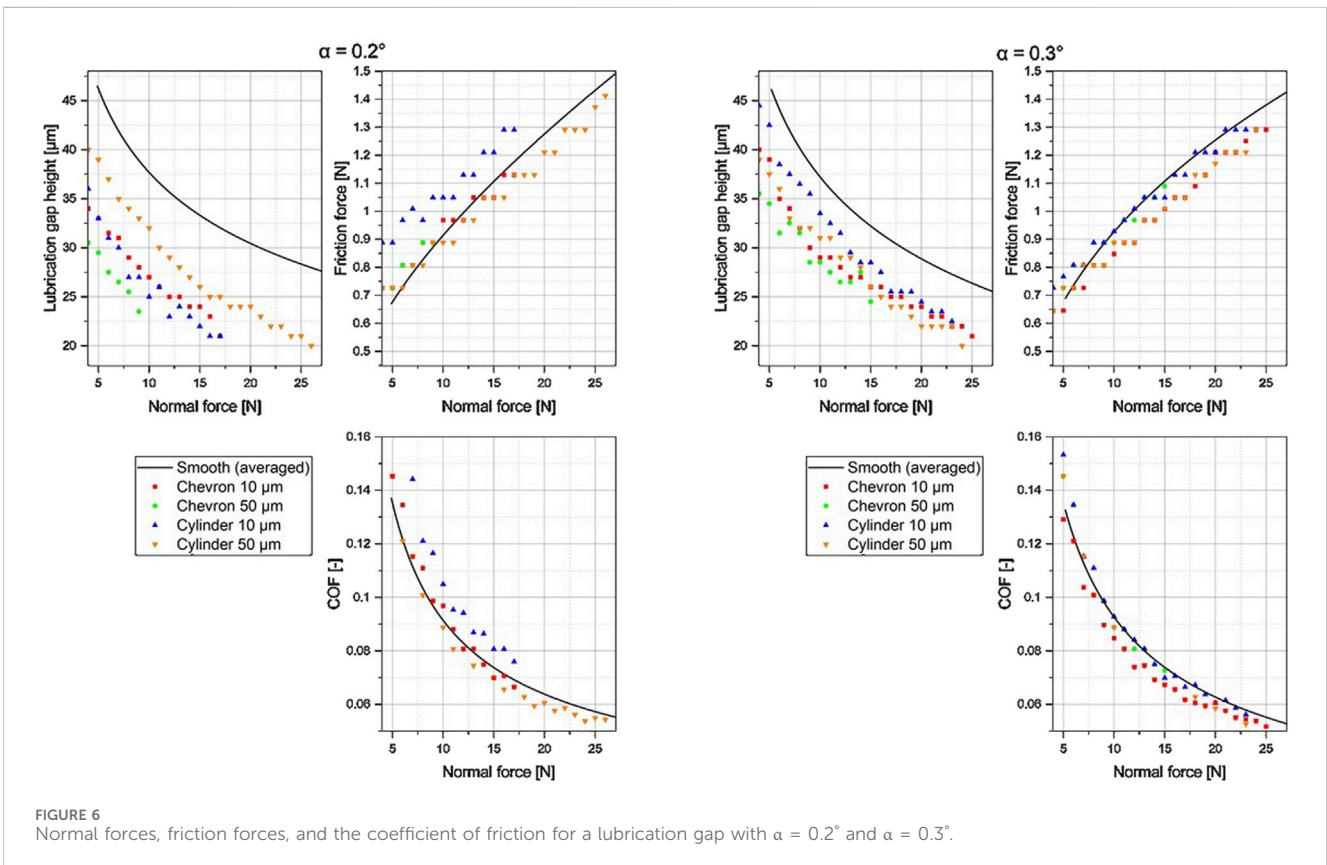
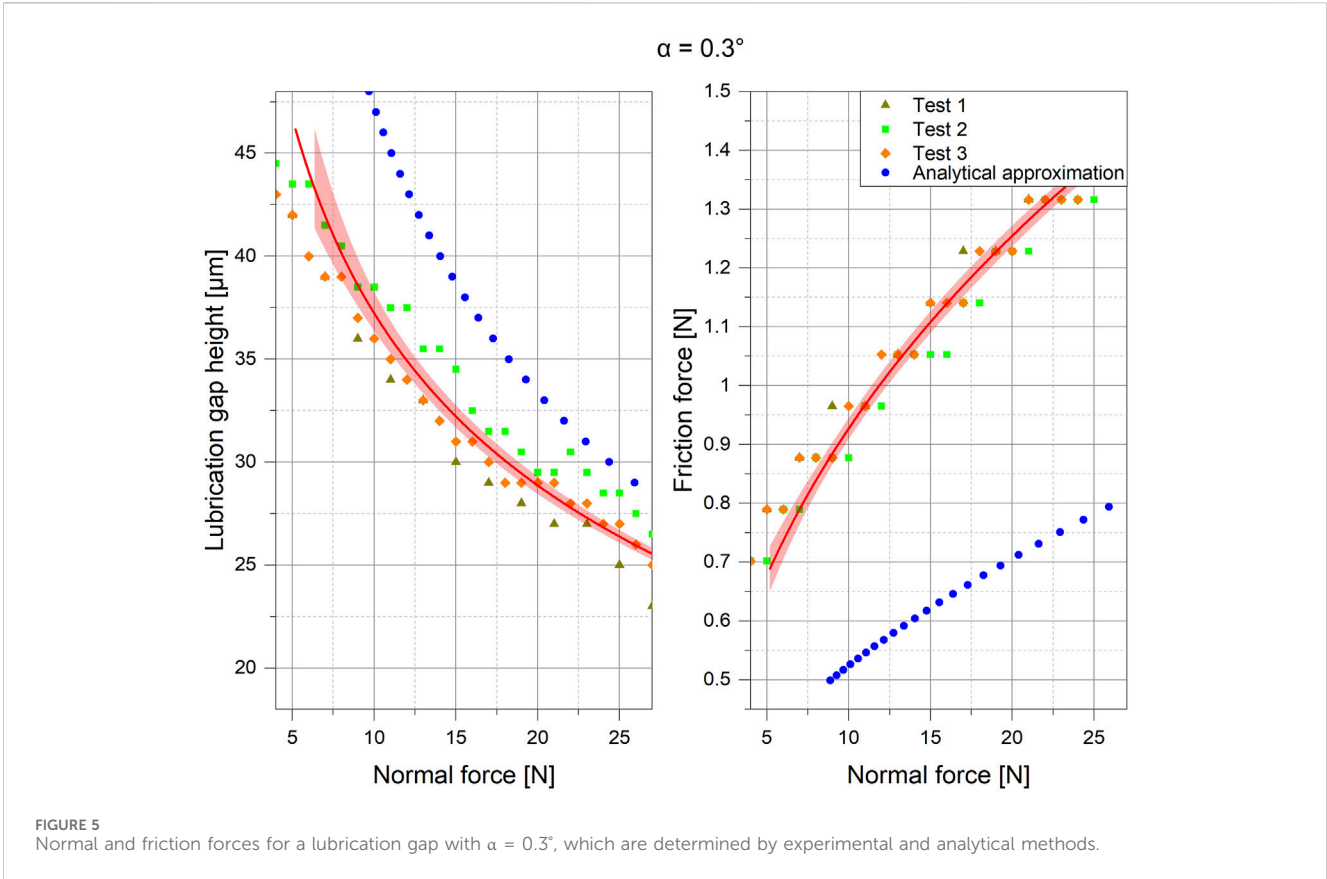


FIGURE 4 Dimensions of the manufactured textures.



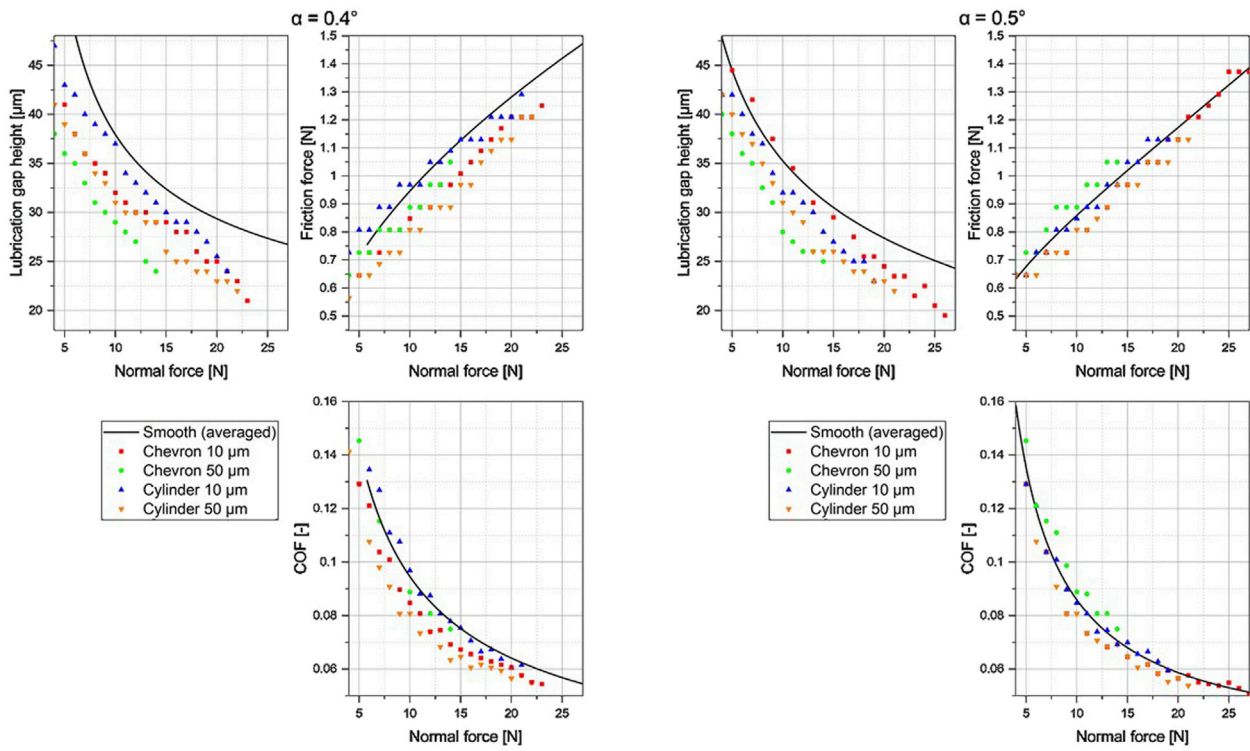


FIGURE 7 Normal forces, friction forces, and the coefficient of friction for a lubrication gap with $\alpha = 0.4^\circ$ and $\alpha = 0.5^\circ$.

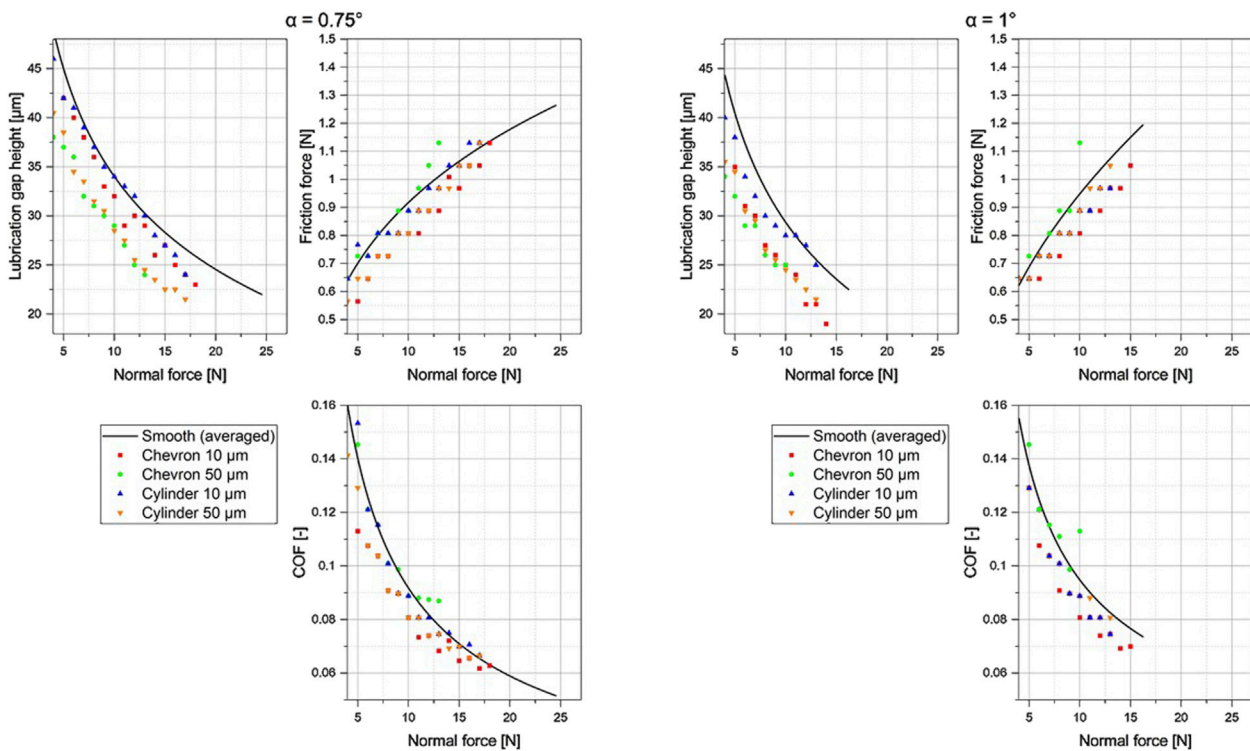


FIGURE 8 Normal forces, friction forces, and the coefficient of friction for a lubrication gap with $\alpha = 0.75^\circ$ and $\alpha = 1.0^\circ$.

force and COF. For friction, the cylinder texture with a depth of 50 μm is the best.

Figure 8 depicts the results of the investigations with pitch angles of 0.75° and 1.0°. For both pitch angles, the cylinder texture with 10- μm depth shows quite similar lubrication gap heights as the smooth reference specimens. In addition, the friction force and COF for this texture are the highest for both pitch angles. Furthermore, it can be observed that for both angles, 0.75° and 1°, the chevron with 10- μm depth provides the lowest COF, so from a frictional point of view, it provides the best enhancement. Particularly, for the investigation at a 0.75° pitch angle, the measured lubrication gap height is quite close to the smooth reference, so the bearing capacity is also good. However, it must be noted that at the higher pitch angles, the overall bearing capacity is significantly reduced, with the maximum reachable normal force being approximately 14 N and the friction forces being less than 1 N for a pitch angle of 1°.

In general, it can be observed that the lubrication gap heights at the same normal forces are lower for the textured specimens than for the smooth specimens. The consequence is a reduction in the friction force and COF, but there is also the risk of operation in the mixed friction regime. Overall, it is difficult to say which texture performs the best. For most cases, the chevron geometry with a depth of 10 μm provides the best compromise between friction reduction and loss of bearing capacity. For some cases (e.g., a pitch angle of 0.75°), the lubrication gap heights of this texture are in the range of the smooth results, indicating a similar bearing capacity but with significant reduction in friction and COF. However, the main finding is that a universal statement is hard to find, and textures need to be designed individually for the specific case of operation.

4 Discussion

In the experimental setups by Azami et al. (2022) and Long et al. (2021) investigating the influence of textures, the lubricating gap height was not measured. With the presented experimental setup of our contribution, it is possible to determine the lubrication gap height during operation by measuring the distance using an eddy current sensor. The innovative measurement configuration enables the characterization of the lubrication gap geometry, in particular, the clear height h_0 as a function of the normal load. This additional information on the lubrication gap height provides insights into the critical load-bearing capacity of textured surfaces. Although textures reduce friction force and the coefficient of friction under most investigated conditions, they also increase the risk of entering the mixed friction regime. This should be considered for potential future applications of friction-reducing textures.

Furthermore, the presented results display the issue of the sensitive and complex behavior of textured, hydrodynamic contacts. The operating conditions under which the texture should be used need to be considered very carefully. A beneficial texture for one operation point cannot guarantee similar improvements for a quite different operation point, as one can also see from the experimental data.

With ongoing texture depth, a reduction in friction force could be observed for most of the investigated cases. One hypothesis for

describing this phenomenon is the increase in lubrication gap height, even if only locally (Maier et al., 2023; Gachot et al., 2017). This would result in a reduced shear gradient, followed by a reduction in the shear force. This would suggest that deeper textures provide even lower shear forces than shallower ones. This can be confirmed for the pitch angles of 0.2°, 0.3°, 0.4°, and 0.5°. For the pitch angles of 0.75° and 1°, the chevron texture with 10- μm depth depicts the lowest friction force, so simply a reduction in the shear gradient cannot be the only explanation for the friction reduction effect of textures.

For nearly all the investigated textures, the deeper ones provide a lower lubrication gap height. One explanation could be that the deeper textures cannot bear the pressure as effectively as the shallower ones.

It is well-known that incorporating textures into a smooth surface disturbs the pressure build-up of the converging wedge. This leads to the reduced gap height and bearing capacity, as observed in nearly all the experiments. New findings in this field suggest that placing textures in the high-pressure region of a bearing always leads to trouble with pressure build-up. Placing textures in the inlet region of a bearing or a converged wedge can lead to a beneficial behavior and can generate an even greater bearing capacity than that of an untextured surface (Scharf et al., 2024b).

However, certain aspects of the method should be critically evaluated and can be improved in the future. By adjusting the pitch angle using the measuring screw on the lever, the initial parallelism and desired lubrication gap angles can be set. A theoretical setting accuracy of the angle of $\Delta\alpha = 0.0073^\circ$ can be achieved by the presented geometry and measuring screw. The key issue in this scenario is that the initial, parallel alignment of the specimens demands special attention during setting with the pressure-sensitive measurement films in order to be able to compare the individual test runs.

The temperature was measured in the test unit. Using an additional measurement, the temperature of the lubricant in the contact area could be determined, and the value for the viscosity could be adapted for the analytical models according to Ubbelohde-Walther (DIN, 2011). For the used oil, the present temperature is in the range of large viscosity gradients. Therefore, small changes in temperature result in rather large changes in viscosity. In order to incorporate the temperature effect on viscosity in the analytical model and ensure better comparability between the experiment and calculation, an *in situ* temperature measurement in the contact area should be included in future work to provide more reliable viscosity values.

These viscosity mismatches could be part of the explanation for a significant difference between the laboratory results of a smooth gap and the analytical solution. A second factor is likely the measurement error of the small friction and normal forces. The SRV test rig is built to apply normal forces up to 2,500 N, and the maximum measured normal forces within this project are 25 N, which is 1% of the maximum. Future improvements should address these problems as well.

However, with the developed test rig, comparable trends between different texture geometries were observed. With further adaptations, the potential for experimental testing of textures could be further exploited.

5 Conclusion and outlook

Within the presented research, the following findings could be found:

- A novel test rig was designed to evaluate the effect of textures on the hydrodynamic load-carrying capacity and frictional force in wedge-shaped lubrication gaps. The distinguishing feature is the additional measurement of the clear lubrication gap height using an eddy current sensor.
- It could be shown that the test rig is capable of differentiating between smooth and various textured specimens in a clear and comprehensive manner for the measured parameters, which were normal and friction force and lubrication gap height.
- Variations in the pitch angle led to different performances of textures. Finally, no single texture could be declared the best performer for all investigated pitch angles, ranging from 0.2° to 1°.
- The benefits of textures can be observed by reducing the hydrodynamic friction force for a wide range of investigated parameters. For most of them, a reduction in the lubrication gap height could be also detected. A higher chance of running into a mixed friction regime needs to be considered.
- In addition, points of very poor performance, characterized by low lubrication gap height combined with higher friction force, can also be found. These types of textures can provide better performance, at least in terms of larger gap height, for a different pitch angle.
- Finally, it needs to be pointed out that the results display the issue that the performance of hydrodynamic textures is strongly dependent on the respective operation conditions and cannot be attributed in a general manner (e.g., this texture is always good).

In future work, sensors could be fitted to the textured pin to extract further data from the experimental test setup. Similar to the work of [Breiteneder et al. \(2019\)](#), information on temperature and hydrodynamic pressure could be derived. Furthermore, to improve the alignment of the parallelism of the pin, a method to rotate the specimen around the longitudinal axis would be desirable.

Subsequently, it is possible to determine surface textures that lead to an enhancement in load-bearing capacity and friction. The

long-term goal is to gain a deeper understanding of the mechanism of textures in order to selectively design textures for performance improvement. Such textures can then improve the performance of bearings, guidances, or other lubricated contacts.

Data availability statement

The raw data supporting the conclusions of this article will be made available by the authors, without undue reservation.

Author contributions

MP: Conceptualization, Supervision, Writing–original draft, Writing–review and editing, Methodology. MM: Writing–review and editing, Methodology. RS: Methodology, Validation, Writing–review and editing. FH: Investigation, Writing–review and editing. FG: Supervision, Writing–review and editing.

Funding

The author(s) declare that no financial support was received for the research, authorship, and/or publication of this article.

Conflict of interest

The authors declare that the research was conducted in the absence of any commercial or financial relationships that could be construed as a potential conflict of interest.

Publisher's note

All claims expressed in this article are solely those of the authors and do not necessarily represent those of their affiliated organizations, or those of the publisher, the editors and the reviewers. Any product that may be evaluated in this article, or claim that may be made by its manufacturer, is not guaranteed or endorsed by the publisher.

References

- Azami, B., Torabi, A., Akbarzadeh, S., and Esfahanian, M. (2022). Experimental investigation of textured surfaces in line and point mixed lubrication contact. *J. Stress Analysis* 6, 59–65. doi:10.22084/jrstan.2022.25913.1202
- Babu, P. V., Ismail, S., and Ben, B. S. (2021). Experimental and numerical studies of positive texture effect on friction reduction of sliding contact under mixed lubrication. *Proc. Institution Mech. Eng. Part J J. Eng. Tribol.* 235, 360–375. doi:10.1177/1350650120930911
- Bijani, D., Deladi, E. L., Akchurin, A., de Rooij, M. B., and Schipper, D. J. (2018). The influence of surface texturing on the frictional behaviour of parallel sliding lubricated surfaces under conditions of mixed lubrication. *Lubricants* 6, 91. doi:10.3390/lubricants6040091
- Breiteneder, T., Schubert-Zallinger, C., Wimmer, A., Vyštejn, J., Hager, G., and Schallmeiner, S. (2019). "Innovative instrumented sliding bearings as a new approach to on-board bearing monitoring," in *ASME 2019 internal combustion engine division fall technical conference* (Chicago, Illinois, USA: American Society of Mechanical Engineers).
- Bukvic, M., Gajević, S., Skulic, A., Savic, S., Asonja, A., and Stojanovic, B. (2024). Tribological application of nanocomposite additives in industrial oils. *Lubricants* 12, 6. doi:10.3390/lubricants12010006
- Chowdhury, H., Loganathan, B., Wang, Y., Mustary, I., and Alam, F. (2016). A study of dimple characteristics on golf ball drag. *Procedia Eng.* 147, 87–91. doi:10.1016/j.proeng.2016.06.194
- de Kraker, A., van Ostayen, R. A. J., and Rixen, D. J. (2010). Development of a texture averaged Reynolds equation. *Tribol. Int.* 43, 2100–2109. doi:10.1016/j.triboint.2010.06.001
- DIN (2011). *Prüfung von Mineralölen und verwandten Stoffen_- Bestimmung des Viskosität-Temperatur-Verhaltens_- Richtungskonstante m*. DIN 51563:2011-04. Berlin: Beuth Verlag GmbH.
- Dobrica, M. B., and Fillon, M. (2009). About the validity of Reynolds equation and inertia effects in textured sliders of infinite width. *Proc. Institution Mech. Eng. Part J J. Eng. Tribol.* 223, 69–78. doi:10.1243/13506501JET433

- Dobrica, M. B., Fillon, M., Pascovici, M. D., and Cicone, T. (2010). Optimizing surface texture for hydrodynamic lubricated contacts using a mass-conserving numerical approach. *Proc. Institution Mech. Eng. Part J J. Eng. Tribol.* 224, 737–750. doi:10.1243/13506501JET673
- Filgueira Filho, I., Bottene, A. C., Silva, E. J., and Nicoletti, R. (2021). Static behavior of plain journal bearings with textured journal - experimental analysis. *Tribol. Int.* 159, 106970. doi:10.1016/j.triboint.2021.106970
- Fowell, M., Olver, A. V., Gosman, A. D., Spikes, H. A., and Pegg, I. (2006). Entrapment and inlet suction: two mechanisms of hydrodynamic lubrication in textured bearings. *J. Lubr. Technol.* 129, 336–347. doi:10.1115/1.2540089
- Fuller, D. D., Maier, W., Paul, H., and Kadmer, E. H. (1960). Theorie und Praxis der Schmierung.
- Gachot, C., Rosenkranz, A., Hsu, S. M., and Costa, H. L. (2017). A critical assessment of surface texturing for friction and wear improvement. *Wear* 372–373, 21–41. doi:10.1016/j.wear.2016.11.020
- Goti, E., Mazza, L., Mura, A., and Zhang, B. (2020). An early method for the technical diagnosis of pin-on-disk tribometers by reference friction measurements in EHL conditions. *Measurement* 166, 108169. doi:10.1016/j.measurement.2020.108169
- Gropper, D., Wang, L., and Harvey, T. J. (2016). Hydrodynamic lubrication of textured surfaces: a review of modeling techniques and key findings. *Tribol. Int.* 94, 509–529. doi:10.1016/j.triboint.2015.10.009
- Grützmacher, P. G., Rosenkranz, A., Szurdak, A., König, F., Jacobs, G., Hirt, G., et al. (2018). From lab to application - improved frictional performance of journal bearings induced by single- and multi-scale surface patterns. *Tribol. Int.* 127, 500–508. doi:10.1016/j.triboint.2018.06.036
- Hamilton, D. B., Walowit, J. A., and Allen, C. M. (1966). A theory of lubrication by microirregularities. *J. Basic Eng.* 88, 177–185. doi:10.1115/1.3645799
- Holmberg, K., and Erdemir, A. (2017). Influence of tribology on global energy consumption, costs and emissions. *Friction* 5, 263–284. doi:10.1007/s40544-017-0183-5
- Lang, O. R., and Steinhilper, W. (2014). *Gleitlager: Berechnung und Konstruktion von Gleitlagern mit konstanter und zeitlich veränderlicher Belastung: mit 6 Arbeitsblättern, Softcover Nachdr. der Orig.-Ausg. nineteenthseventheighth*. Berlin: Springer.
- Leitl, P. A., Stenzel, V., Flanschger, A., Kordy, H., Feichtinger, C., Kowalik, Y., et al. (2020). *Riblet surfaces for improvement of efficiency of wind turbines*. Orlando, FL: AIAA Scitech 2020 Forum.
- Liu, W., Ni, H., Chen, H., and Wang, P. (2019). Numerical simulation and experimental investigation on tribological performance of micro-dimples textured surface under hydrodynamic lubrication. *Int. J. Mech. Sci.* 163, 105095. doi:10.1016/j.ijmecsci.2019.105095
- Liu, W., Ni, H., Wang, P., and Zhou, Y. (2020). An investigation on the drag reduction performance of bioinspired pipeline surfaces with transverse microgrooves. *Beilstein J. Nanotechnol.* 2020, 24–40. doi:10.3762/bjnano.11.3
- Long, R., Zhao, C., Zhang, Y., Wang, Y., and Wang, Y. (2021). Effect of vein-bionic surface textures on the tribological behavior of cylindrical roller thrust bearing under starved lubrication. *Sci. Rep.* 11, 21238. doi:10.1038/s41598-021-00800-x
- Luo, Y., Yuan, L., Li, J., and Wang, J. (2015). Boundary layer drag reduction research hypotheses derived from bio-inspired surface and recent advanced applications. *Micron* 79, 59–73. doi:10.1016/j.micron.2015.07.006
- Maier, M., Pusterhofer, M., and Grün, F. (2023). Multiscale wear simulation in textured, lubricated contacts. *Coatings* 13, 697. doi:10.3390/coatings13040697
- Milojevic, S., Glisovic, J., Savic, S., Boskovic, G., Bukvic, M., and Stojanovic, B. (2024). Particulate matter emission and air pollution reduction by applying variable systems in tribologically optimized diesel engines for vehicles in road traffic. *Atmosphere* 15, 184. doi:10.3390/atmos15020184
- Milojevic, S., Savic, S., Maric, D., Stopka, O., Kristic, B., and Stojanovic, B. (2022). Correlation between emission and combustion characteristics with the compression ratio and fuel injection timing in tribologically optimized diesel engine. *Teh. Vjesn.* 29. doi:10.17559/TV-20211220232130
- Milojevic, S., Savic, S., Mitrovic, S., Maric, D., Kristic, B., Stojanovic, B., et al. (2023). Solving the problem of friction and wear in auxiliary devices of internal combustion engines on the example of reciprocating air compressor for vehicles. *Teh. Vjesn.* 30. doi:10.17559/TV-20220414105757
- Milojevic, S., and Stojanovic, B. (2018). Determination of tribological properties of aluminum cylinder by application of Taguchi method and ANN-based model. *J. Braz. Soc. Mech. Sci. Eng.* 40, 571. doi:10.1007/s40430-018-1495-8
- Mishra, P., and Ramkumar, P. (2018). “Effect of micro texture on tribological performance of piston ring-cylinder liner system under different lubrication regimes,” in *International conference on advances in design, materials, manufacturing and surface engineering for mobility* (Chennai, India: SAE International).
- Morris, N., Leighton, M., de La Cruz, M., Rahmani, R., Rahnejat, H., and Howell-Smith, S. (2015). Combined numerical and experimental investigation of the micro-hydrodynamics of chevron-based textured patterns influencing conjunctural friction of sliding contacts. *Proc. Institution Mech. Eng. Part J J. Eng. Tribol.* 229, 316–335. doi:10.1177/1350650114559996
- Olver, A. V., Fowell, M. T., Spikes, H. A., and Pegg, I. G. (2006). Inlet suction’, a load support mechanism in non-convergent, pocketed, hydrodynamic bearings. *Proc. Institution Mech. Eng. Part J J. Eng. Tribol.* 220, 105–108. doi:10.1243/13506501JET168
- Optimol Instruments Prüftechnik GmbH (2024). SRV5 betriebsanleitung gerät.
- Pusterhofer, M., Summer, F., Wuketich, D., and Grün, F. (2019). Development of a model test system for a piston ring/cylinder liner-contact with focus on near-to-application seizure behaviour. *Lubricants* 7, 104. doi:10.3390/lubricants7120104
- Rosenkranz, A., Costa, H. L., Profito, F., Gachot, C., Medina, S., and Dini, D. (2019). Influence of surface texturing on hydrodynamic friction in plane converging bearings - an experimental and numerical approach. *Tribol. Int.* 134, 190–204. doi:10.1016/j.triboint.2019.01.042
- Sahlin, F., Glavatskih, S. B., Almqvist, T., and Larsson, R. (2005). Two-dimensional CFD-analysis of micro-patterned surfaces in hydrodynamic lubrication. *J. Lubr. Technol.* 127, 96–102. doi:10.1115/1.1828067
- Scharf, R., Maier, M., Pusterhofer, M., and Grün, F. (2024a). A comprehensive numerical study of a wedge-shaped textured convergent oil film gap. *Lubricants* 12, 121. doi:10.3390/lubricants12040121
- Scharf, R., Pusterhofer, M., Gussmagg, J., and Grün, F. (2024b). An investigation into the optimal dimple geometry in a single-dimple sliding contact. *Machines* 12, 622. doi:10.3390/machines12090622
- Schiebel, A., and Körner, K. (1933). *Die Gleitlager (Längs-und Querlager): Berechnung und Konstruktion*. Berlin, Heidelberg: Springer.
- Skulic, A., Bukvic, M., Gajevic, S., Miladinovic, S., and Stojanovic, B. (2024). The influence of worm gear material and lubricant on the efficiency and coefficient of friction. *tribomat Tribol. Mater.* 3, 15–23. doi:10.46793/tribomat.2024.001
- Vlădescu, S.-C., Fowell, M., Mattsson, L., and Reddyhoff, T. (2019). The effects of laser surface texture applied to internal combustion engine journal bearing shells - an experimental study. *Tribol. Int.* 134, 317–327. doi:10.1016/j.triboint.2019.02.009
- Vogelpohl, G. (1967). *Betriebsichere Gleitlager: Berechnungsverfahren für Konstruktion und Betrieb, secondnd*. Springer Berlin Heidelberg.
- Wu, L., Wang, J., Luo, G., Wang, S., Qu, J., Fan, X., et al. (2021). Study on the drag reduction characteristics of the surface morphology of *Paramisgurnus dabryanus* loach. *Coatings* 11, 1357. doi:10.3390/coatings11111357
- Zhang, M., Feng, S., Wang, L., and Zheng, Y. (2016). Lotus effect in wetting and self-cleaning. *Biotribology* 5, 31–43. doi:10.1016/j.biotri.2015.08.002